Geomathematical Study of Sandstones Overlying the Phoenix Uranium Deposits and the REE-rich Maw Zone, Athabasca Basin, Saskatchewan

Shishi (Chris) Chen[1], Keiko Hattori[1], Eric C. Grunsky[2] and Yongxing Liu[3]

1. Department of Earth Sciences, University of Ottawa, 25 Templeton Street, Ottawa, Ontario, K1N 6N5
2. Geological Survey of Canada, 601 Booth Street, Ottawa, Ontario, K1A 0E8
3. Denison Mines Corporation, 230 22nd Street East, Suite 200, Saskatoon, Saskatchewan, S7K 0E9

Abstract

To evaluate the relationship between the enrichment of REEs and U mineralization, we carried out Principal Component Analysis (PCA) of sandstones above the Phoenix U deposits and in the REE-rich Maw Zone in the eastern Athabasca Basin. The Phoenix deposits, with indicated resources of 70.2 M lbs U_3O_8, occur along the unconformity and a steeply dipping fault in the basement at ca. 400 m depth. The Maw Zone, a breccia pipe with surface exposure of 300 by 200 m, consists of highly silicified, hematitized, dravitic tourmaline-rich rocks with high REE (<8.1 wt. % as total REE oxides). The Maw Zone is ca. 4 km southwest from the south end of Phoenix deposits and does not contain high U (< 7.8 ppm U) contents. PCA of sandstones above the Phoenix deposits shows that U is associated with Heavy REEs (HREE)+Y, Light REEs (LREE) and Pb, and inversely correlated with Ti, Zr, Al, and Th. The Maw Zone displays different element groupings as revealed by PCA: U is strongly correlated with V, Cr, Fe, Ni, Cu, Cd, Na, Li and Ba, but very weakly correlated with HREEs+Y, and inversely with LREEs and P. Relative enrichment of HREEs, Y, and P suggests xenotime is the predominant host of the HREEs. The grouping of LREEs+Sr+Th+P suggests the occurrence of monazite and/or aluminum phosphate-sulphate (APS) minerals. A mineralogical study confirmed xenotime and APS minerals as the major host of HREEs and LREEs, respectively. These REE-bearing minerals precipitated from hydrothermal fluids during the brecciation of hematitized sandstones. The positive association between U and Fe in the PCA plot from the Maw Zone suggests that U was transported by oxidized fluids. The absence of U mineralization in the Maw Zone is explained by low U in the oxidizing fluids, or a lack reducing fluids to precipitate U.

Introduction

The Athabasca Basin is a large Paleo- to Mesoproterozoic sandstone basin that occupies much of the northernmost quarter of Saskatchewan and a smaller portion of northeastern Alberta. The Phoenix deposits are typical of sandstone-hosted unconformity-related U deposits in the basin (e.g. Kerr, 2010) which can host significant concentrations of rare earth elements (REE) due to their ability to substitute for uranium (U) in the ore mineral uraninite (Fayek and Kyser, 1997; Hanly and Hagni, 2002). The rare earth element-enriched Maw Zone is located only 4 km southwest of the Phoenix deposits but lacks high U contents (< 7.8 ppm U; Denison Mines Corp., 2006). Despite some features in common, such as hematite, xenotime, tourmaline and euhedral quartz alteration assemblages in the sandstone host rocks, the relationship between the two types of mineralization is not clear (Quirt et al., 1991). Previous studies have proposed the Maw Zone is a near-surface expression of processes that also resulted in unconformity-related U mineralization (McDougall, 1990; Hanly, 2001). Using the methodology outlined by Grunsky (2010), principal component analysis (PCA) was applied to evaluate the behavior of elements in sandstones overlying the Phoenix U deposits and those in the REE-rich Maw Zone. First introduced by Pearson (1901), PCA can reduce the dimensionality of a dataset with a large number of variables, while retaining as much as possible of the variation in the variables (Jolliffe, 1986). Further refinements in PCA methodology resulted in the creation of the biplot (Gabriel (1971) that combines the loadings of the variables with the scores of the observations on the same dia-

gram. The reduction in the number of variable to describe the variation in the data and the association of the variable facilitates recognition of geological processes responsible for these variables, with several geoscientific applications such as: elemental assemblages associated with geochemical processes, hydrothermal alteration and mineralization (Grunsky, 1986) and evaluation of mineral assemblages in regional stream sediment geochemical data and styles of mineralization (Grunsky et al., 2009; Grunsky, 2010). This paper presents the results of PCA from two deposits located close to each other with different styles of mineralization, compares the elemental assemblages of the two, and discusses the processes important for controlling the U and REE mineralization in each system.

General study area

The study area is located in the eastern Athabasca Basin (Fig. 1). The Maw Zone is located ca. 4 km southwest of the southern end of the Phoenix uranium deposits along the same northeast-trending structure, the WS shear.

Sandstone stratigraphy

In the study area, the Athabasca Basin is comprised of sandstones and conglomeratic sandstones of the Manitou Falls and Read Formations. Three members of the Manitou Falls Formation are recognized, using the parameters of Ramaekers et al. (2007) and are presented in Table 1. The thickness of sandstones overlying the Phoenix deposits is ca. 450 m whereas the total thickness of sandstones at the Maw Zone varies greatly from 202 m in the western part, to over
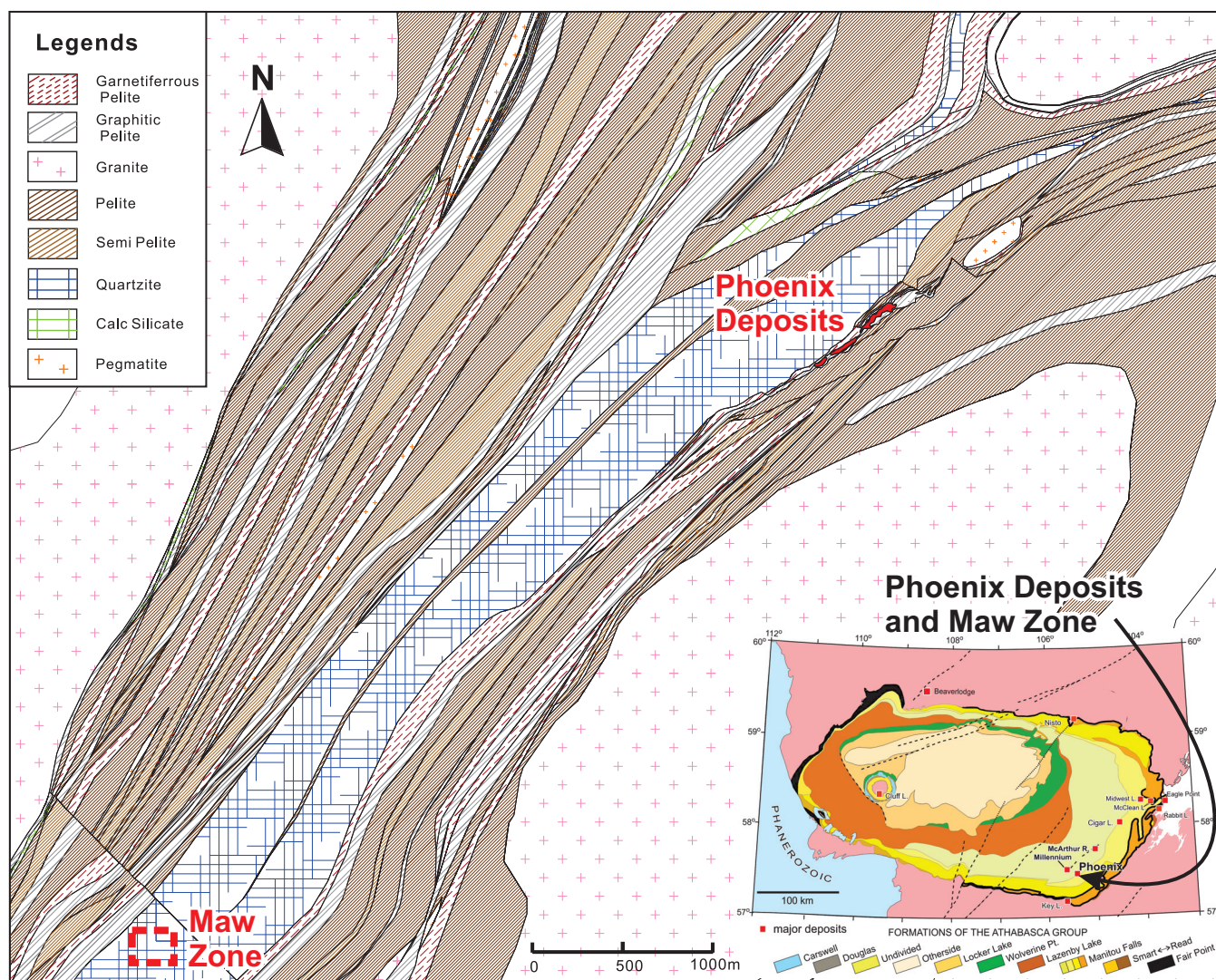
FIGURE 1. Basement geological map of the Wheeler River Property illustrating the location of the Maw Zone 4 km southwest of the Phoenix Deposit Zone B (Denison Mines Corp., 2014). Inset: Location of the study area within the Athabasca Basin, northern Saskatchewan (after Jefferson et al., 2007).

TABLE 1. Athabasca Group units in the study area, using classification of Ramaekers et al. (2007).

	Unit (from top to bottom)	Lithology
Manitou Falls Formation	Dunlop Member (MFd)	Fine-grained quartz arenite with abundant (>1 vol. %) clay intraclasts
	Collins Member (MFc)	Quartz arenite with rare (<1 vol. %) clay intraclasts
	Bird Member (MFb)	Interbedded quartz arenite and conglomerate distinguished from the underlying Read Formation and overlying MFc by the presence of at least 1 % to 2 vol. % conglomerate in beds thicker than 2 cm
Read Formation (formerly the MFa Member)		Sequence of poorly sorted quartz arenite and minor conglomerate

300 m in east and north (Denison Mines Corporation, 2006). The large difference in the sandstone thickness is partly due to the presence of a quartzite ridge that was a paleotopographic high prior to deposition of the Athabasca Group but was also displaced by fault reactivation syn- and post-depo-

sition of the sandstones, as noted from the McArthur River and Phoenix deposits (Marlatt et al., 1992; Györfi et al., 2007; Jefferson et al., 2007; Ramaekers et al., 2007; Tourigny et al., 2007; Yeo et al., 2007; Kerr, 2010). A major northeast-trending basement fault directly below the Maw

Geomathematical Study of Sandstones Overlying the Phoenix Uranium Deposits and the REE-rich Maw Zone, Athabasca Basin, Saskatchewan

Zone occurs along a metapelite unit in quartzite, with significant vertical displacement and moderate to steep dip to the east. Sandstones and quartzite close to the fault are brecciated (Barker, 2011).

Phoenix uranium deposits

The Phoenix deposits are unconformity-type uranium deposits lying along the unconformity between the Athabasca Group sandstones and Paleoproterozoic basement rocks at ca. 450 m of depth (Kerr, 2010). Current indicated resources are 70.2 million lbs U_3O_8 at an average grade of 19.13 % U_3O_8 (Roscoe, 2014). Minor amounts of ore also extend from the unconformity into the basement along the WS Shear Zone. Alteration in the sandstones above the deposits is characterized by the formation of kaolinite-group minerals, illite, and dravitic tourmaline (Dann et al., 2014). Basement rocks at the Phoenix deposit are part of the Wollaston Domain and are comprised of metasedimentary and granitoid gneisses. The metasedimentary rocks belong to the Wollaston Supergroup and include graphitic and non-graphitic metapelitic and semipelitic gneisses, meta-quartzite, and rare calcsilicate rocks together with felsic and quartz feldspathic granitoid gneisses (Roscoe, 2014). The basement geology is similar to the Maw Zone and is critical to the unconformity-related U models.

The Maw Zone (REE)

The Maw Zone, with a surface exposure of 300 by 200 m, consists of highly silicified, hematitized, dravitic tourmaline-rich rocks with high REE and Y concentrations (up to 8.1 wt. % as total REE oxides; Agip Canada Ltd, 1985). Despite similar alteration assemblages, host rocks, and proximity to the uranium deposits (Fig. 1), the zone does not contain significantly concentrations of U (< 7.8 ppm U); except for one sample located close to the unconformity at a depth of 320 m (DDH-WR195 with 40.9 ppm U). The most prominent feature of the Maw zone is the intensely brecciated and altered Athabasca sandstones, including large (40 to 90 cm) cross-bedded clasts (McDougall, 1990). The predominant crystalline basement rocks are a succession of variably graphitic, sillimanite-, garnet- and cordierite-bearing, biotite metapelites, semipelites and quartzite (Barker, 2011).

Methodology

Principal Component Analysis

This study applied R (variables or elements in this study)-Q (samples) mode Principal Component Analysis scripts developed by Grunsky (2001) in the R statistical software environment (R Core Team, 2013), and described in detail in Chen et al. (2014). In general, PCA is a multivariate procedure to reduce the dimensionality of a multivariate dataset to a smaller set of summary components, while retaining as much as possible of the variation in the original variables (Jolliffe, 1986). For the Phoenix and Maw Zone datasets, RQ-mode PCA appears to be well-suited for evaluating the elemental association and geological processes associated with the geochemical dataset because it can display the relationships of the samples and elements at the same scale. After a centered log-ratio transformation of the raw data, the elemental assemblages were evaluated using simultaneous RQ-mode PCA. As geochemical data are governed by the stoichiometry of minerals, the elemental assemblages can represent minerals (Grunsky et al., 2008). Geochemical data are compositional in nature and therefore restricted in the positive number space (simplex). Statistics applied to such data are not valid and the use of logratios are required to "open" the data into the real number space in which statistics can be properly applied (Aitchison, 1986). In this study the centred logratio was applied to all of the data prior to any statistical analysis.

Geochemical Datasets

This study uses chemical compositions of sandstones determined at the Saskatchewan Research Council for Denison Mines Corp. using inductively coupled plasma optical emission spectrometry (ICP-MS) and inductively coupled plasma mass spectrometry (ICP-OES) following near total digestion of samples using three acids (HF-HNO$_3$-HCl). Complete details on the analytical methods can be found in Roscoe (2014). The size of the two datasets and chemical elements used for PCA are listed in Table 2.

Mineralogical Study

Thirty-eight polished thin sections were made from the Maw Zone and 60 from Phoenix site for petrography. They were examined with a petrographic microscope and a JEOL 6610 LV scanning electron microscope (SEM) equipped with an Oxford SDD detector at University of Ottawa.

Results

Sandstones overlying the Phoenix deposits

Sample and variable scores derived from PCA are projected onto the PC1-PC2 axes of Figures 2A and B. The two Principal Components (PC1 and PC2), explain 40.2% of the total variation in the data. The figure shows distinct groupings of elements in four sandstone units. Relative enrichment of U-HREE-Y-Pb occurs along the positive PC1 axis in RD, MFc and MFd units. Relative enrichment of LREE occurs exclusively in the RD, along the positive PC1 and PC2 axes. The enrichments of U and REE are inversely associated with Fe-Mn-Th-Ti-Al-K.

The biplot of PC2-PC3 (accounting for 18.0% of the total variation) shows LREE enrichment along the positive PC2 axis; mostly in the RD and MFb (Figs. 2B, D). The HREEs and Y occur together with high-field strength elements Zr, Hf, Nb, and Th along the negative PC3 axis; mostly in MFc although the element association is weak, with only small number of samples exhibiting this feature (Fig. 2B). This pattern is also expressed weakly for MFb and RD.

Scores of PC1 and PC2 for the data from the RD were plotted in Figure 3. The biplot indicates that there is a relative enrichment of U, Y and HREEs along the positive PC1 axis (Fig. 3A). This enrichment is inversely associated with relative enrichment of K-Fe-Al-Mg-Mn-Ca-Ni-Ga-Zn, which have negative scores of PC1 (Fig.3A). The biplot of PC1-PC2 shows that U is not associated with REEs in the MFb, as relative enrichment of REEs is shown along the

TABLE 2. Summary of the Phoenix deposits and Maw Zone datasets. Some of the elements were removed from the dataset because concentrations below or close to their detection limits.

	Total number of samples	Number of sandstone samples	Analytical method	Elements used for PCA	Elements removed from dataset	Rare Earth Elements
Phoenix	6718	4630	ICP-OES	Al, Ba, Be, Ca, Cd, Ce, Cr, Cu, Dy, Er, Eu, Fe, Ga, Gd, Hf, Ho, K, La, Li, Mg, mn, na, Nb, Nd, Ni, P, Pb, Pr, Sr, Th, Ti, U, V, Y, Yb, Zn, Zr, B, Sm	Ag, Co, Mo, Sc, Sn, Ta, Tb and W	La, Ce, Pr, Nd, Sm, Eu and Gd (LREE) Dy, Yb, Er and Ho (HREE)
Maw Zone	660	545	ICP-MS	U, Cu, La, Fe, Ni, P, Pb, V, Y, Zn, Al, Ba, Be, Ca, Cd, Ce, Cr, Dy, Er, Eu, Ga, Gd, Hf, K, Li, Mg, Na, Nb, Nd, Pr, Sc, Sm, Sr, Th, Ti, Yb	Ag, Co, Mo, Sn, Ta, Tb, and W	La, Ce, Nd, and Sm (LREE) Dy, Yb, Er, and Gd (HREE)

positive PC1 axis without U (Fig. 3B). There is a positive association of HREE and high-field strength elements (Th-Zr-Ti-Nb). The MFc data shows a weak relative enrichment of U-Pb-Y-HREEs- Hf-Zr and Ni-Na-B-Mg along the positive PC1 axis (Fig. 3C). The biplot of PC1-PC2 for MFd (Fig. 3D) shows relative enrichment of HREEs along the negative PC1 axis and LREEs along the positive PC2 axis. In the MFd, U and Pb are not associated with REEs. Relative U-Pb enrichment is weakly associated with positive PC5 scores (not shown).

Vertical stratigraphic profile of the principal components

When the scores of the first and second principal components are plotted stratigraphically (Fig. 4) , the RD unit generally displays higher PC1 and PC2 scores than upper sandstone units, although there is greater dispersion of RD relative to the other units. Elements in decreasing order of dominance in PC1 are: K, Dy, Er, Fe, Y, Mn, Yb, U, and Th. Elements in decreasing order of dominance in PC2 are: V, Mg, Nd, Sm, P, Sr, Ce, La, Pr, Ni and B. Uranium appears as a dominant element in PC1 together with HREEs and LREEs in PC2. Therefore, PC1 and PC2 represent relative enrichment of U and REEs in the sandstones overlying the Phoenix deposits. Furthermore, U shows positive values in PC1 and PC2 scores, therefore, samples with high positive values of PC1 and PC2 are likely associated with the enrichment of U. The findings may be useful in evaluating the potential for uranium deposits in the area by mapping PC1 and PC2 scores of rocks by interpolation.

Sandstones of the Maw Zone

Relative enrichment of HREEs and Y is observed along the negative PC2 axis in samples from the MFb, MFc and MFd in PC1 vs. PC2 plot (Fig. 5A). These two PCs account

for 36.3% of the total information. Figure 5A also shows the separation of HREEs and LREEs, and the fractionation of Eu from the rest of the REE. Sandstones in the Maw Zone show negative Eu anomalies compared to Sm and Gd. LREE enrichment along PC1 and the position of P between HREEs and LREEs suggest that samples contain at least two phosphate phases: HREE-rich xenotime and LREE-rich monazite. The enrichment of Fe is observed in the upper left quadrant in Figure 5A, reflecting hematite which is abundant in all rocks in the Maw Zone. Therefore, the enrichment of Fe is attributed to the presence of an oxidized environment. The PC1 and PC2 loadings for Fe show a distinct location in the upper left quadrant of Figure 5A. This indicates that the concentrations of Fe are relatively higher in rocks plotted towards the upper left quadrant. The sandstone samples plotted towards the upper left are interpreted to be more oxidized.

PC3 and PC4 together account for 18.0% of the total variance. The biplot of PC3 versus PC4 shows that the samples with a relative enrichment in U, LREEs, and P plot along the positive axis of PC3 (Fig. 5B), indicating the likely association of LREEs with monazite or possibly APS minerals. Since U concentrations are low in the Maw Zone, U in monazite may explain this elemental association.

Principal component analysis of the Maw Zone data shows that Sr, Th, Y, the LREEs, Ti, V and U, contribute mostly to the variation of PC1, and the HREEs, P, Y Li, Ni and Ba for PC2. The 3D diagrams of drill holes and scores of PC1 and PC2 of total dataset (Fig. 6) shows negative scores of PC1 and PC2 appear in the upper part of sandstones (MFc and MFd). Since the HREEs and Y show strongly negative scores on PC2, this reflects the occurrence of xenotime in the upper sandstone units.
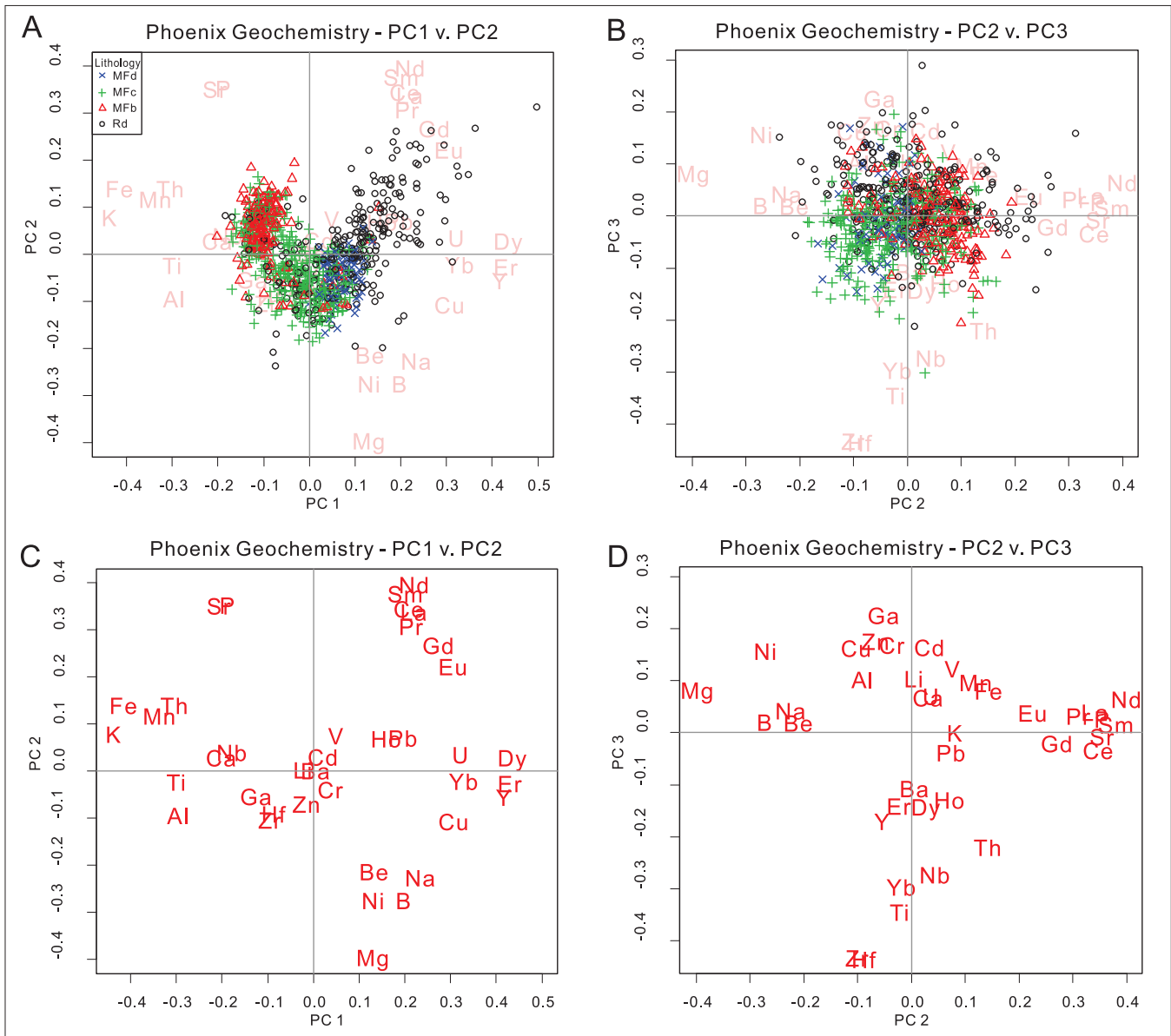
FIGURE 2. Biplots of PC1 vs. PC2 and PC2 vs. PC3 for the combined sandstones dataset for the Phoenix zone. For the clarity of diagrams, elements are separately shown in C and D. The data were transformed using logcentred ratio.

Minerals containing REE in the Maw Zone

In the Maw Zone, REEs are correlated with P, indicating that monazite, APS and xenotime are the potential carriers of REEs. This is consistent with earlier reports on the occurrence of xenotime and monazite by Quirt et al. (1991) and Hanly (2001). Thin section examination shows REE-bearing minerals are concentrated in buff-colored veinlets that cut hematitized fragments of sandstones. The occurrence suggests that REEs were introduced by reduced fluids that dissolved hematite. Back-scattered electron (BSE) images of xenotime show two different occurrences. Subhedral to euhedral grains of xenotime are spatially associated with detrital zircon grains (Figs. 7A, B, C, F, H). The second type is dissemination in a groundmass of sudoite without any zircon grains (Fig. 7G). The fine-grained xenotime appears to

have crystallized late from the hydrothermal fluids. In addition, several small (< 5 μm) grains containing high HREEs and Y were noted. They nucleated on zircon grains and show no P contents in energy-dispersive spectra (EDS) on the SEM. The contents of HREEs and Y are much greater than those of xenotime, suggesting that these grains are most likely the REE carbonate bastnäsite (Figs. 7D, E).

Aluminum phosphate-sulphate minerals were identified as the primary host of LREEs in the Maw Zone. Monazite was not found in our samples. The APS minerals occur as aggregates of small grains in sandstone (Fig. 7A) and in a matrix of magnesio-foitite ± sudoite and illite (Fig 8). Analysis of EDS from the APS minerals indicates that they contain elevated Sr and LREE contents. They also contain SO_4^{2-} and Ca, suggesting that the APS minerals are most likely solid
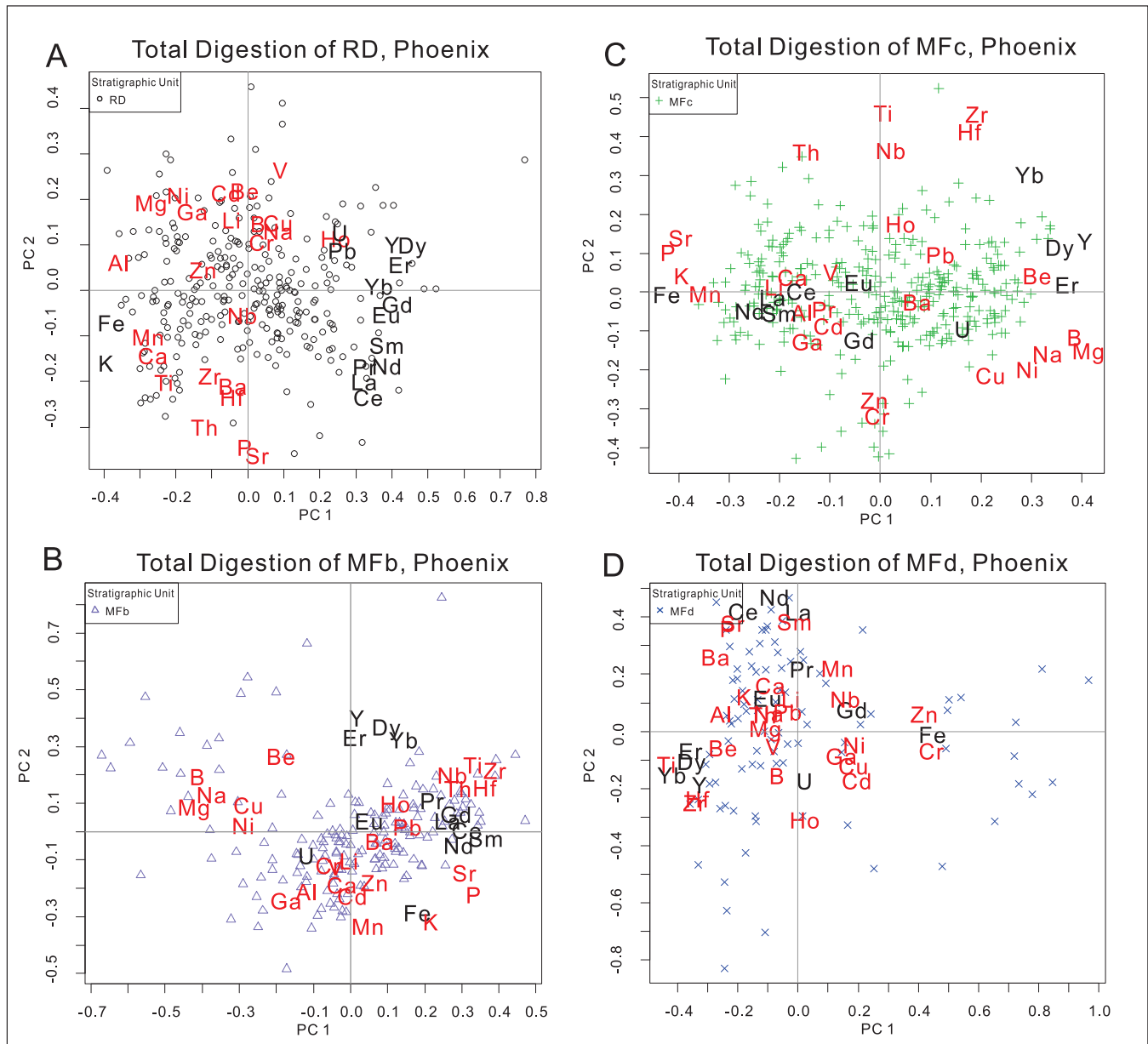
FIGURE 3. Biplots of PC1 vs. PC2 for the RD, MFb, MFc and MFd datasets separately for sandstones overlying the Phoenix deposits. The data were transformed using logcentred ratio.

solutions of svanbergite-florencite. The presence of SO_4^{2-} confirms the oxidized environments for the hydrothermal activity. Core of APS minerals are known to contain high Th (Mwenifumbo and Bernius, 2007). The association of Th and LREE in PCA is consistent with Th hosted by APS minerals.

Discussion and Summary

The PCA shows distinct geochemical signatures in the different sandstone units above the Phoenix deposits: relative enrichment of LREEs, HREEs and Y in RD; P, Sr, Th, Mn, K and Fe in MFb; Ca, Nb, Ti, Al, Zr, and Zn in MFc, Na, B, Ni, Mg and Cr in MFd.

For Maw Zone dataset, most of the relative HREE and Y enrichments occur in MFd and MFc and LREE in RD, MFb and MFc samples. Relative enrichment of HREEs and Y-P occur in the MFb, MFc and MFd samples.

The sandstones above the Phoenix deposits show that U is associated with HREEs+Y, LREEs and Pb, and inversely correlated with Ti, Zr, Hf, Al, and Th. The relative enrichment of K-Fe-Al-Mg-Mn-Ca-Ni-Ga-Zn, which have negative scores of PC1 (Fig.3A), likely reflects the presence of Fe-oxides, sudoite and illite. These minerals are common in altered sandstones overlying the unconformity deposits (Jefferson et al., 2007 and references therein). The location of Ca along the negative PC1 axis may reflect the presence of
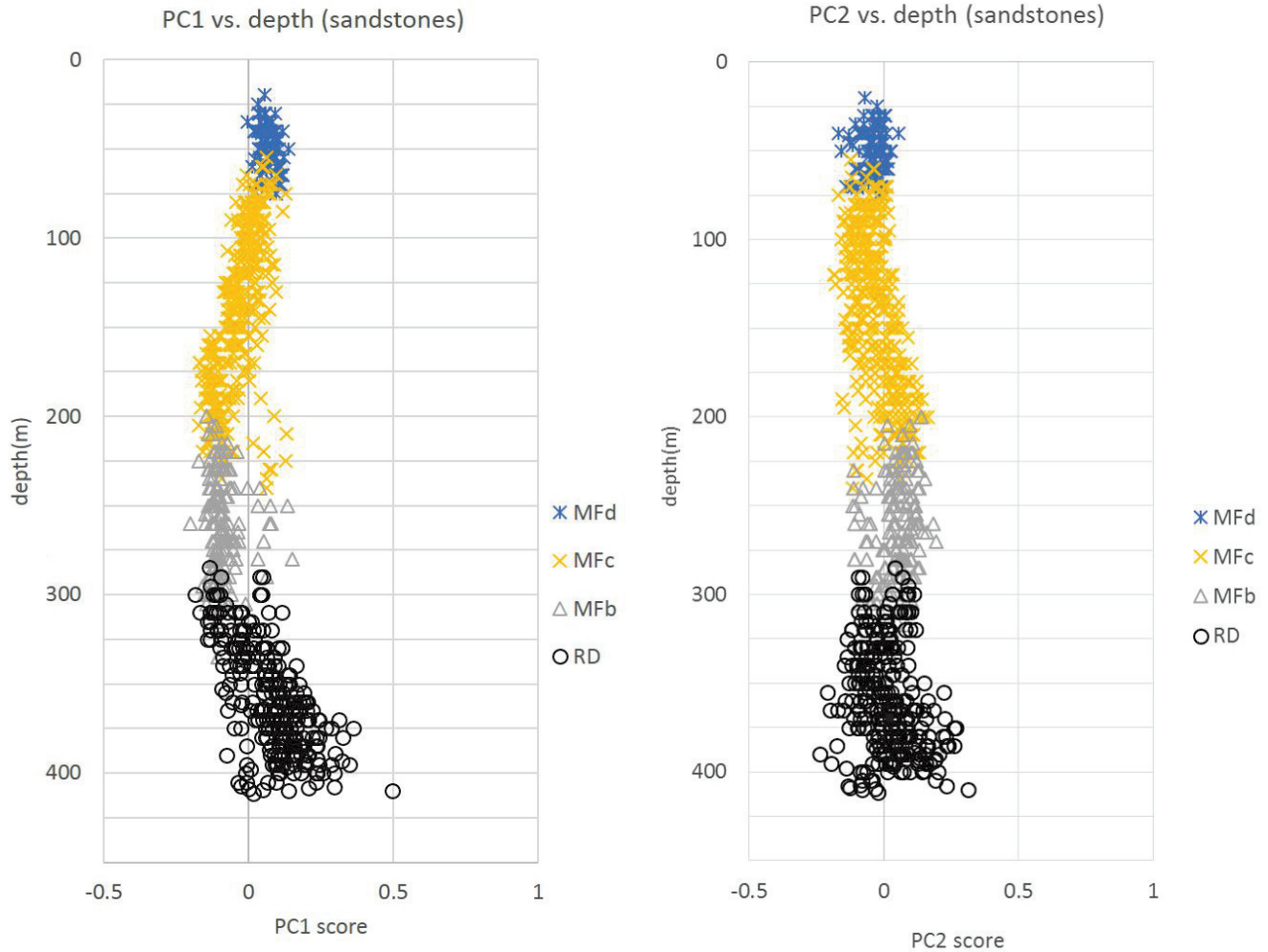
FIGURE 4. Plots of vertical variations of PC1 and PC2 scores in sandstones over the Phoenix deposit. The data were transformed using logcentred ratio.

unaltered feldspar or calcite-dolomite veins. This will be confirmed in further petrographic studies. The positive association of HREE and high-field strength elements (Th-Zr-Ti-Nb) may reflect the presence of heavy minerals, such as zircon and oxides. This will be confirmed through a mineralogical study of samples. The MFc data shows a weak relative enrichment of U-Pb-Y-HREEs- Hf-Zr and Ni-Na-B-Mg along the positive PC1 axis (Fig. 3C), supporting an association of U and REEs with tourmaline (B-Na-Mg, most likely magnesio-foitite) in the MFc. The tourmaline has high vacancy in the X-site and relatively high Mg, and is classified as magnesiofoitite (O'Connell et al., 2015). Uranium is inversely correlated with Zr, Hf and Th but positively correlated with HREEs. Zircon grains can contain high concentrations of not only HREEs and Y but also Zr, Hf and Th (Föster, 2006). However, the observed elemental association suggests that zircon is not an important host of REEs in the sandstones. Furthermore, P is closely associated with REEs, Al and Sr, therefore APS may be important host. Although REEs are associated with U in the sandstone above the Phoenix deposits, the absolute concentrations are overall low

($\sum$REEs <150 ppm) and it was difficult to identify phases hosting REEs.

Compared with the Phoenix dataset, the Maw Zone has different element groups: U is strongly correlated with V, Cr, Fe, Ni, Cu, Cd, Na, Li and Ba, but very weakly correlated with HREEs+Y, and inversely with LREEs and P. Relative enrichment of HREEs and Y-P suggests that xenotime is the predominant host of the HREEs while the elemental grouping of LREEs-Sr-Th-P in the MFb suggests the occurrence of monazite and/or APS minerals. The mineralogical studies confirmed APS minerals as the major host of LREEs.

The positive correlation between U and Fe and their loadings in the oxidized regions of the biplots suggest that U was transported by oxidized fluids and is associated with Fe-oxides (possibly adsorbed on Fe-oxides/hydroxides and clays). REEs and U have different precipitation mechanisms, with U reduced from relatively soluble U^{6+} to insoluble U^{4+} in a reducing environment (Jefferson et al., 2007). Deposition of REEs is related to increasing pH and decreasing temperature (Williams-Jones et al., 2012)]. Although REEs can be transported by oxidizing brines similar to those which trans-
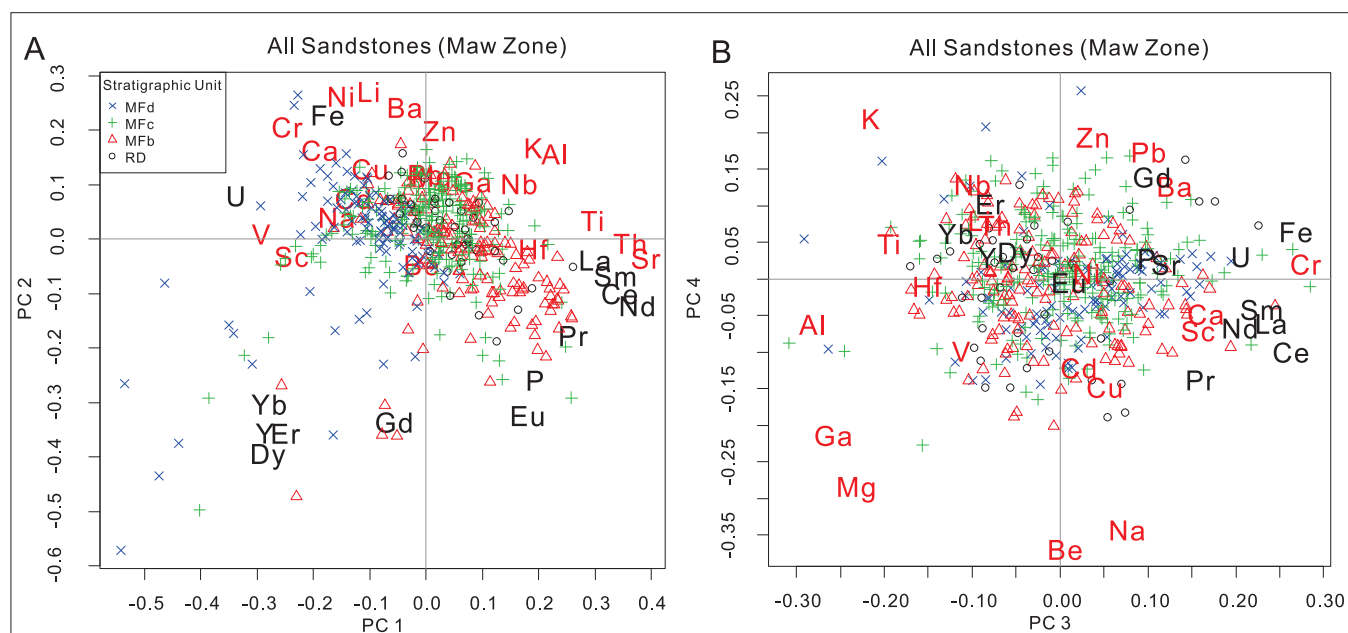
FIGURE 5. Biplots of PC1 vs. PC2 and PC3 vs. PC4 for all sandstone data from the Maw Zone. The data were transformed using logcentred ratio.
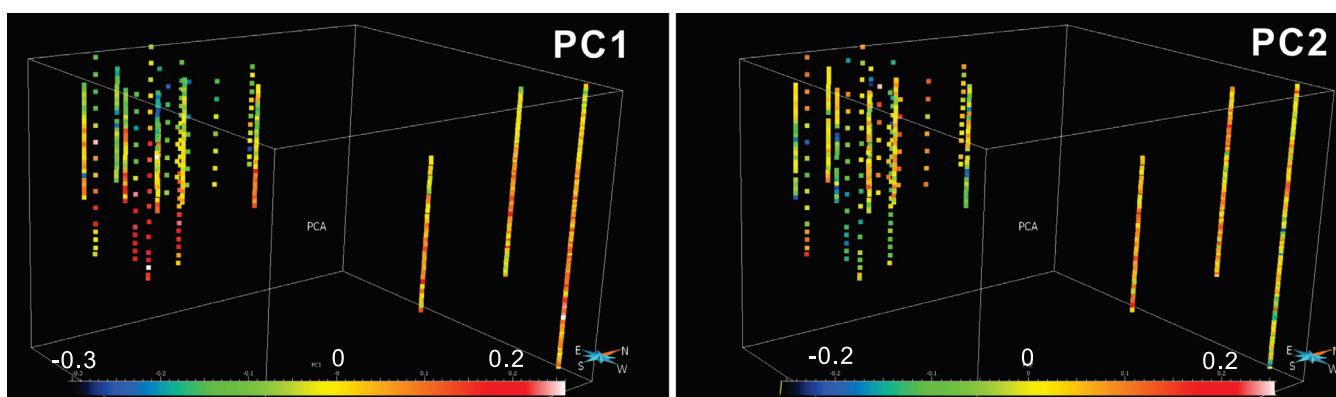

FIGURE 6. 3D diagrams showing scores of PC1 (Left) and PC2 (Right) in drill cores. The data were transformed using logcentred ratio.

port U (Fayek and Kyser, 1997), if there is no reducing conditions, REEs may precipitate while U remains in the fluids.

Sandstones in the Maw Zone show negative Eu anomalies compared to Sm and Gd, suggesting interaction between hydrothermal fluids and felsic rocks. Ca-rich plagioclase is the major host of Eu^{2+} and mafic igneous rocks commonly show positive Eu anomalies in chondrite-normalized REE patterns, whereas felsic rocks show negative Eu anomalies in normalized patterns because of earlier crystallization of plagioclase in mafic rocks (Henderson, 1984)

Uranium concentrations in the Maw Zone are overall low (< 7.89 ppm U in almost all samples; Denison Mines Corp., 2006), although the values are generally higher than the average crustal concentration of 0.91 ppm U (Taylor and McLennan, 1985). Uranium shows positive correlations with Fe, V and Cr (Fig. 5A), suggesting that relatively high contents of U are associated with Fe oxides (possibly adsorbed on Fe-oxides/hydroxides and clays). The data suggests that

small quantities of U precipitated under oxidized conditions. Since rocks of MFd are mostly plotted in the upper left quadrant, it is interpreted that the MFd unit was less reduced or not reduced compared to MFb and MFc. This is reasonable considering that the MFd is the farthest unit from the reduced basement rocks. The occurrence of kaolinite with Fe oxides in the MFd suggests that this oxidation likely took place during the diagenesis of sandstones.

There are three possible explanations for the absence of significant U mineralization in the Maw Zone. The concentrations of U in the oxidizing fluids were low, as suggested by Pan et al. (2013) based on the lack radiation-induced defects in quartz. Alternatively, the oxidizing fluids did not encounter reduced fluids or media in the basement to precipitate U. Finally, introduction of REEs in reduced fluids took place at much later time, as shown by REE-rich veins in the hematite-rich breccia.
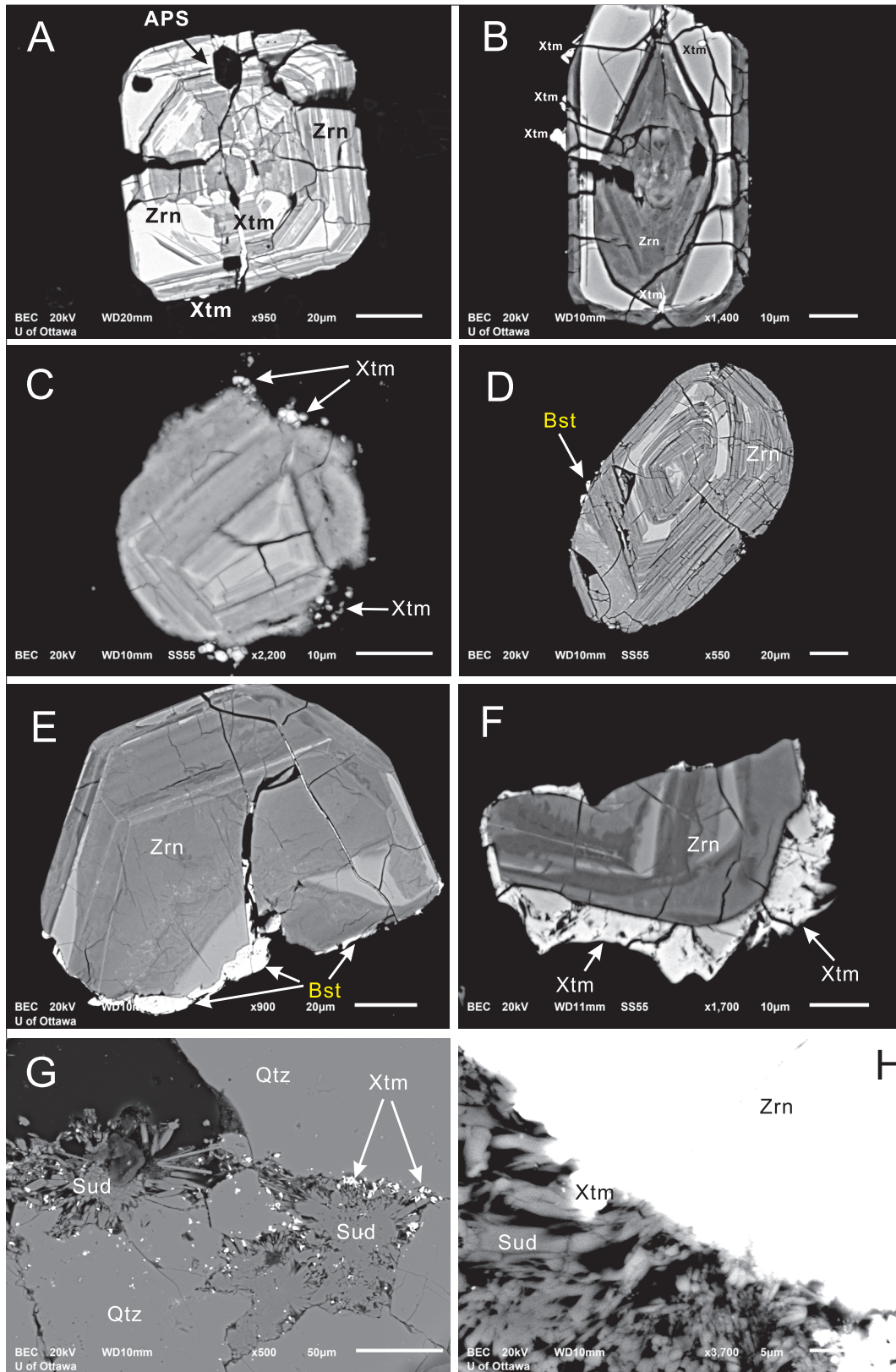
FIGURE 7. Backscatter electron (BSE) images of xenotime (Xtm) and bastnäsite (Bst) in sandstone samples from MFb (Fig. 7A: DDH 85-3, 102.5m depth, Fig 7B and H: ZQ-09, 215m depth, Fig. 7G: DDH 85-3, 132.5m depth), MFd (Fig 7C: DDH 84-2, 30m depth; Fig 7D: DDH 84-2, 50m depth), the RD (Fig 7E: ZQ-09 225m depth, Fig 7F: DDH WR-194, 357.5m depth). Bst = bastnäsite, Mgf= magnesiofoitite, Qtz = quartz, Sud = Sudoite, Xtm = xenotime, Zrn = zircon.
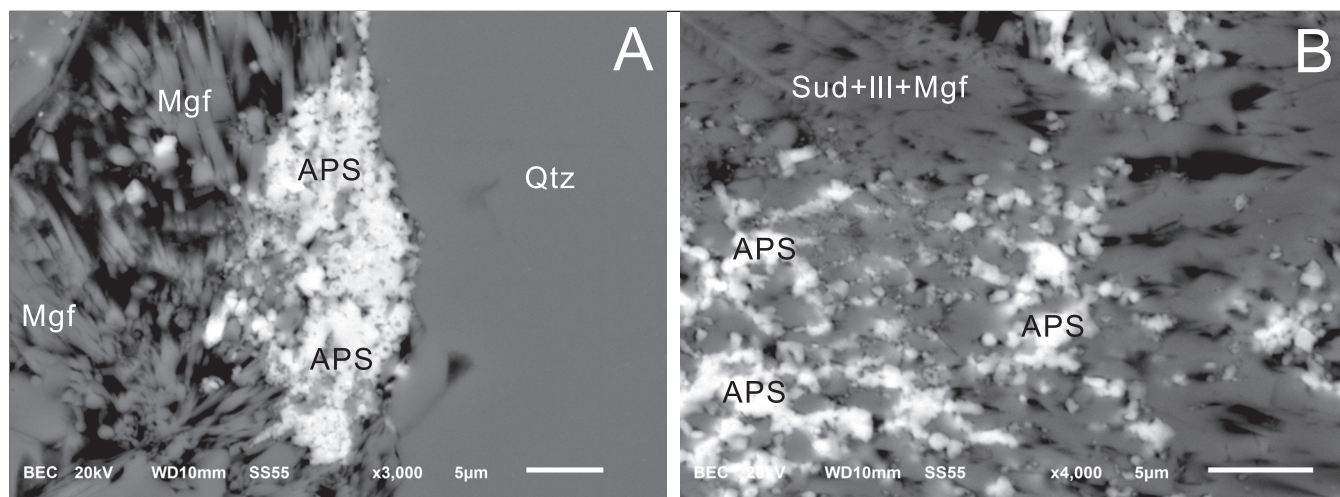
FIGURE 8. BSE images of APS minerals (bright) in sandstone sample from MFd (DDH ZQ-08, 33 m depth). Ill=illite, Mgf = magnesiofoitite, alkali-deficient Mg-rich tourmaline, Qtz=quartz.

Exploration Implications

The elemental assemblages observed from dominant PCs are likely associated with alteration assemblages. Therefore, these elemental associations can be used to recognize alteration related to unconformity-related uranium deposits. In this study, positive values in PC1 and PC2 scores are associated with the enrichment of U. These findings may be useful in evaluating the potential for U deposits in the area by mapping PC1 and PC2 scores of rocks by interpolation.

Acknowledgments

References

Agip Canada Ltd., 1985. Assessment File 74H06-NW-0080: Saskatchewan Ministry of Energy and Mines, 113 p.

Aitchison, J., 1986. The statistical analysis of compositional data. Chapman and Hall, New York. 416p.

Barker, M., 2011. The Y and HREE enrichment of the Maw Zone, Wheeler River preliminary Summary; unpublished report prepared for Denison Mines Corporation, 16 p.

Chen, S., Grunsky, E., Hattori, K., and Liu, Y., 2014. Principal component analysis of geochemical data from the REE-rich Maw Zone, Athabasca Basin, Canada; Geological Survey of Canada, Open File 7689, 22 p.

Dann, J., Hattori, K., Potter, E.G., and Sorba, C., 2014. Discrimination of Elemental Assemblages in the Alteration Halo of the Phoenix Deposit, Saskatchewan, Through Applied GIS; Geological Survey of Canada, Open File 7463. 66 p.

Denison Mines Corporation, 2006. [Geochemistry of the REE-enriched Maw Zone]; Unpublished raw data.

Denison Mines Corporation, 2014. Wheeler River Property; <http://www.denisonmines.com/s/Wheeler_River.asp>

Fayek, M., and Kyser, T.K., 1997. Characterization of multiple fluid-flow events and rare earth element mobility associated with formation of unconformity- type uranium deposits in the Athabasca basin, Saskatchewan; The Canadian Mineralogist, v. 35, p. 627–758.

Föster, H.-J., 2006. Composition and origin of intermediate solid solutions in the system thorite–xenotime–zircon–coffinite; Lithos v. 88, p. 35-55.

Gabriel, K.R., 1971. The biplot graphic display of matrices with application to principal component analysis; Biometrika, v. 58, p. 453–467.

Grunsky, E.C., 1986. Recognition of alteration in volcanic rocks using statistical analysis of lithogeochemical data; Journal of Geochemical Exploration, v. 25, p. 157–183.

Grunsky, E.C., 2001. A program for computing RQ-mode principal components analysis for S-plus and R; Computers and Geosciences, v. 27, p. 229–235.

Grunsky, E.C., Drew, L.J., and Sutphin, D.M., 2009. Process recognition in multi-element soil and stream-sediment geochemical data; Applied Geochemistry, v. 24, p. 1602–1616.

Grunsky, E.C., Kjarsgaard, B.A., Egozcue, J.J., Pawlowsky-Glahn, V., and Thió i Fernández de Henestrosa, S., 2008. Studies in Stoichiometry with Compositional Data; in Proceedings of CODAWORK'08, 7 p.

Grunsky, E.C. 2010. The interpretation of geochemical survey data; Geochemistry, Exploration, Environment Analysis, v. 10, p. 27–74.

Györfi, I., Hajnal, Z., White, D.J., Takács, E., Reilkoff, B., Annesley, I.R., Powell, B., and Koch, R., 2007. High-resolution seismic survey from the McArthur River region: contributions to mapping of the complex P2 uranium ore zone, Athabasca Basin, Saskatchewan; in EXTECH IV: Geology and Uranium Exploration TECHnology of the Proterozoic Athabasca Basin, Saskatchewan and Alberta, (ed.) C.W. Jefferson and G. Delaney; Geological Survey of Canada, Bulletin 588, p. 397–412.

Hanly, A.J., 2001. The mineralogy, petrology and rare earth element geochemistry of the Maw Zone, Athabasca Basin, Canada, University of Missouri-Rolla; unpublished M.Sc. thesis, 108 p.

Hanly, A.J., and Hagni, R.D., 2002. The petrology and rare earth element geochemistry of the Maw Zone: an yttrium and heavy rare earth element enriched zone in the Athabasca Basin, Canada; Joint Annual meeting of the Geological Association of Canada – Mineralogical Association of Canada, Abstracts, v. 27, 1 p.

Henderson, P., 1984. Rare earth element geochemistry. Elsevier. 510 p.

Jefferson, C.W., Thomas, D.J., Gandhi, S.S., Ramaekers, P., Delaney, G., Brisbin, D., Cutts, C., Portella, P., and Olson, R.A., 2007. Unconformity-associated uranium deposits of the Athabasca Basin, Saskatchewan and Alberta; in EXTECH IV: Geology and Uranium EXploration TECHnology of the Proterozoic Athabasca Basin, Saskatchewan and Alberta, (ed.) C.W. Jefferson and G. Delaney; Geological Survey of Canada Bulletin 588, p. 23–68

Jolliffe, I.T., 1986. Principal Component Analysis; Encyclopedia of Statistics in Behavioral Science, John Wiley & Sons, Ltd, 487 p.

Kerr, W.C., 2010. The discovery of the Phoenix Deposit; a new high-grade, Athabasca Basin unconformity-type uranium deposit, Saskatchewan, Canada; Society of Economic Geologists Special Publications, v.15, p. 703–728.

Marlatt, J., McGill, B., Matthews, R., Sopuck, V., and Pollock, G., 1992. The discovery of the McArthur River uranium deposit, Saskatchewan, Canada; in New Developments in Uranium Exploration, Resources, Production and Demand; International Atomic Energy Agency and the Nuclear Energy Agency of the Organization for Economic Cooperation Development, IAEA-TECDOC-650, p. 118–127.

McDougall, D.G., 1990. Rare earth element mineralization in the Athabasca Group – Maw Zone; in Summary of Investigations 1990; Saskatchewan Geological Survey, Miscellaneous Report 90-4, 3 p.

Mwenifumbo, C.J., and Bernius, G.R., 2007. Crandallite-group minerals: host of thorium enrichment in the eastern Athabasca Basin, Saskatchewan; in EXTECH IV: Geology and Uranium Exploration TECHnology of the Proterozoic Athabasca Basin, Saskatchewan and Alberta, (ed.) C.W. Jefferson and G. Delaney; Geological Survey of Canada Bulletin 588, p. 521–532.

O'Connell, I., Hattori, K., Chen, S., Adlakha, E.E., and Sorba, C., 2015. Tourmaline in the Maw Zone, uranium ore of the Gryphon Zone and sandstones above the Phoenix uranium deposits, Athabasca Basin, Saskatchewan, Canada; Presentation at Saskatchewan Geological Open House 2014, 1 poster.

Pan, Y., Yeo, G., Rogers, B., Austman, C., and Hu, B., 2013. Application of natural radiation-induced defects in quartz to uranium exploration: A case study on the Maw Zone, Athabasca Basin; in Uranium in Canada: Geological Environments and Exploration Developments, (ed.) E.G. Potter, C.W. Jefferson and D. Quirt; Journal of Exploration and Mining Geology, v. 21, p. 115–128.

Pearson, K., 1901. On lines and planes of closest fit to systems of points in space; Philosophical Magazine, v. 11, p. 559–572.

Quirt, D., Kotzer, T., and Kyser, T.K., 1991. Tourmaline, phosphate minerals, zircon and pitchblende in the Athabasca Group: Maw Zone and McArthur River areas; in Summary of Investigations 1991; Saskatchewan Geological Survey, Saskatchewan Energy and Mines, Report 91-4, p. 181–191.

Ramaekers, P., Jefferson, C.W., Yeo, G.M., Collier, B., Long, D.G.F., Drever, G. and Wheatley, K., 2007. Revised geological map and stratigraphy of the Athabasca Group, Saskatchewan and Alberta; in EXTECH IV: Geology and Uranium Exploration TECHnology of the Proterozoic Athabasca Basin, Saskatchewan and Alberta, (ed.) C.W. Jefferson and G. Delaney; Geological Survey of Canada Bulletin 588, p. 155–190.

R Core Team., 2013. R: A Language and Environment for Statistical Computing; R Foundation for Statistical Computing, Vienna, Austria. <http://www.R-project.org/>.

Roscoe, W., 2014. Technical report on a mineral resource estimate update for the Phoenix uranium deposit, Wheeler River Project, eastern Athabasca Basin, Northern Saskatchewan, Canada; NI 43-101 technical report, 134 p.

Taylor, S.R., and McLennan, S.M., 1985. The Continental Crust: Its Composition and Evolution; Blackwell Scientific Publications, 328 p.

Tourigny, G., Quirt, D.H., Wilson, N.S.F., Wilson, S., Breton, G., and Portella, P., 2007. Geological and structural features of the Sue C uranium deposit, McClean Lake area, Saskatchewan; in EXTECH IV: Geology and Uranium Exploration TECHnology of the Proterozoic Athabasca Basin, Saskatchewan and Alberta, (ed.) C.W. Jefferson and G. Delaney; Geological Survey of Canada, Bulletin 588, p. 229–247.

Williams-Jones, A.E., Migdisov, A.A., and Samson, I.M., (2012). Hydrothermal mobilization of the rare earth elements – a tale of 'ceria' and 'yttria'. Elements, v. 8, p. 355-360

Yeo, G.M., and Delaney, G., 2007. The Wollaston Supergroup, stratigraphy and metallogeny of a Paleoproterozoic Wilson cycle in the Trans-Hudson Orogen, Saskatchewan; in EXTECH IV: Geology and Uranium Exploration TECHnology of the Proterozoic Athabasca Basin, Saskatchewan and Alberta, (ed.) C.W. Jefferson and G. Delaney; Geological Survey of Canada, Bulletin 588, p. 89–118.